Journal of the Korean Society of Oceanography
Vol. 38, No. 2, pp. 45 — 51 June 2003

A simple Model for Separation of the Tsushima Current Stream Core by the Tsushima Island: a small viscosity limit

YOUNG HO SEUNG
Department of Oceanography, Inha University, Inchon 402-751, Korea

Recent observations reveal that the Tsushima Current has a double-cored structure downstream of the Tsushima Island. To explain this, a simple analytical model is proposed based on the assumption of small lateral eddy viscosity. This model suggests that an otherwise uniform current becomes to have a stream core immediately after it enters a channel due to the action of lateral friction. The core is initially broad but becomes sharper downstream. The speed at which the core develops depends on the intensity of lateral eddy viscosity. Likewise, a single-cored stream changes rapidly to a double-cored stream when it passes through an island located in the center of the channel. When the stream leaves the island behind, the reverse process from the double- to single-cored structures takes place. In this case, however, the double-cored structure is retained for a significant distance from the island. Overall, this model suggests that the double-cored structure of the Tsushima Current observed downstream of the Tsushima Island is created by the lateral friction exerted by the Tsushima Island.

Key words: Tsushima Current in Korea Strait, Stream core

INTRODUCTION

The Tsushima Current is a unique warm current entering the East Sea (or Japan Sea). It is known to be divided into two major branches after entering the East Sea. One is the East Korean Warm Current (EKWC) flowing northward along the Korean coast, which then separates from the coast after encountering with southward flowing cold current. The other consists of the currents flowing either along the Japanese coast (Nearshore Branch, briefly NB) or along the continental slope further offshore (Offshore Branch, briefly OB). These currents supply warm water mostly to the southern half of the East Sea, hence forming a subpolar front with cold water further north, and are considered to be very important in controlling the oceanographic conditions of the East Sea.

The Korea Strait, the entrance of the East Sea for the Tsushima Current, is a narrow and shallow channel connecting the shallow East China Sea and the much deeper East Sea (Fig. 1). The strait is about 150 km wide and 50–150 m deep and is divided by the Tsushima Island into two sub-channels, the eastern and western channels. The western channel is narrower but deeper than the eastern channel.

In earlier times, attempts have been made to estimate the volume transport through the Korea Strait indirectly by using the sea level difference or by geostrophic dynamic computation (Yi, 1966 and 1970; Kawabe, 1982a; Toba *et al.*, 1982). With the development of oceanographic instruments, current in the Korea Strait is nowadays directly measured with current meters or drifting buoys (Miita and Ogawa, 1984; Mizuno *et al.*, 1989; Egawa *et al.*, 1993; Katoh, 1994; Isobe *et al.*, 1994; Katoh *et al.*, 1996). Thanks to these observations, more detailed knowledges could be obtained about the Tsushima Current passing through the Korea Strait, such as a counterflow on the east side of the Tsushima Island, relatively strong tidal currents with the speed approaching 50 cm/s embedded in the Tsushima Current, and so on. According to these observations, current is strongest (or transport is maximum) in summer and weakest (or transport is minimum) in winter. Recently, Teague *et al.* (2002) performed an extensive current measurements in the Korea Strait. Bottom-mounted ADCP's were moored along two sections, one in the north of the Tsushima Island (section N) and the other in the south of the island (section S), for about one year (Fig. 1). Their results generally agree with traditional knowledges

*Corresponding author: seung@inha.ac.kr

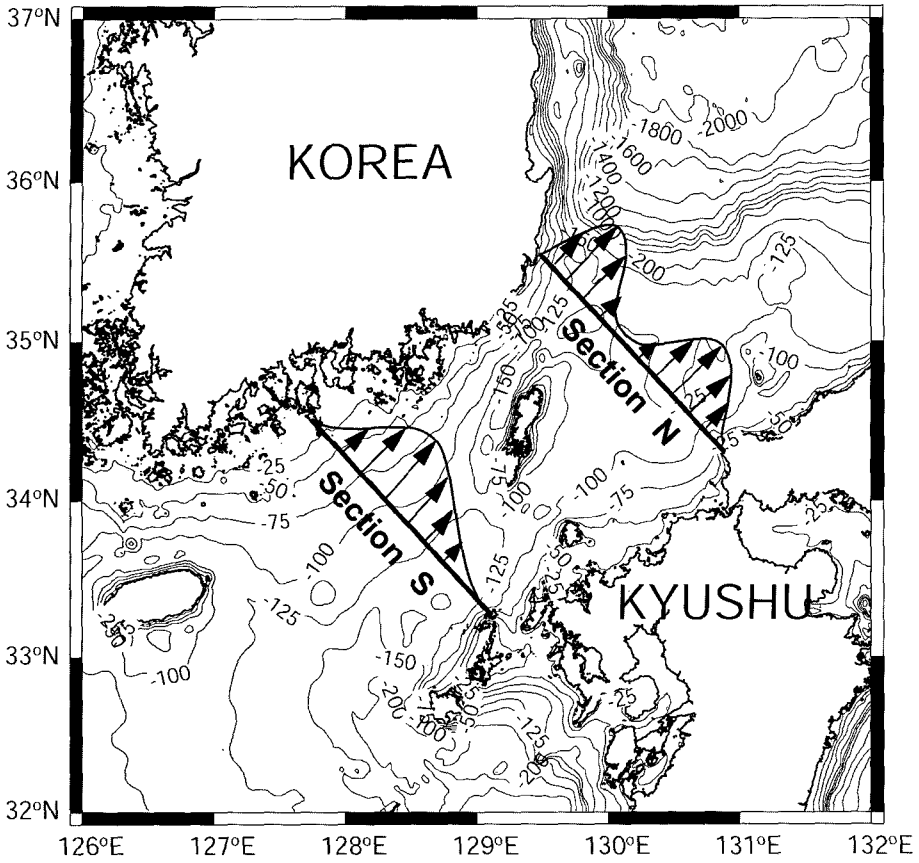

Fig. 1. The Korea Strait with bottom topography (depth in meters). Current profiles along the sections S and N are schematically shown according to Teague *et al.* (2002).

about the Tsushima Current but they indicate strongest current (maximum transport) in October and weakest current (minimum transport) in December. Among others, an interesting feature found in their measurements is that the Tsushima Current has one stream core in the upstream (south) of the Tsushima Island but two cores in the downstream (north) of the island, and a counter current commonly exists in the lee of the island.

Teague *et al.* (2002) simply conjecture that the separation of the stream core is possibly induced by the effect of the Tsushima Island, without giving any theoretical explanation. The aim of this paper is thus to propose a simple analytical model which can clearly explain the physical process of the stream core separation.

FORMULATION

Consider an infinitely long channel of a uniform depth H and width $2L_x$. Take a right-handed cartesian coordinate with x-axis in the cross-channel direction and y-axis in the along-channel direction, with origin at the center of the channel (Fig. 2). In the absence

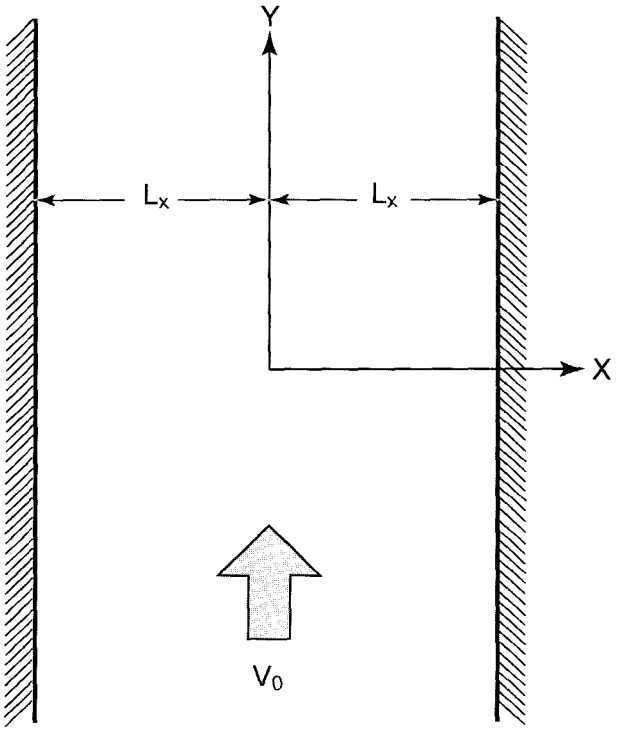

Fig. 2. Configuration of the model channel with coordinate axis. In the absence of lateral friction, a uniform geostrophic current with speed V_0 flows along the channel.

of lateral friction, a uniform geostrophic current with velocity V_o flows along the channel (referred to as "basic flow"), that is

$$fV_0 = g\frac{\partial \eta_0}{\partial x} \tag{1}$$

where f is the Coriolis parameter, g is the gravity constant and η_0 is the basic state surface elevation assumed negligibly small compared with the channel depth. In the channel, the velocity distribution of the basic flow is perturbed by the effect of horizontal eddy viscosity. For small eddy viscosity, one expects narrow regions in the vicinities of the channel walls of width negligibly small compared with L_x, where current velocity decreases rapidly toward zero on the walls. Hereafter, these regions are referred to as "boundary layers". In the region outside the boundary layers, however, the velocity perturbations to that of basic flow is negligibly small, say, of order εV_o or smaller, where ε is a number much smaller than unity. This region of small velocity perturbation is the region of interest in this paper, and hereafter is referred to as "interior region". In the interior region, the velocity perturbation is maximum at outer edges and decreases toward the center of the channel; the velocity perturbations in the interior region vary on a length scale of order L_x. Since the channel length is much larger than the width, velocity changes in y-direction can be assumed much slower than those in x-direction, namely, $L_x \sim \varepsilon L_y$ where L_y is the along-channel length scale of the perturbations (The order of magnitude of L_y will later be estimated.) For constant V_0, the system is under steady state.

With the above setting, the continuity equation reads

$$\frac{\partial u}{\partial x} + \frac{\partial v}{\partial y} = 0 \tag{2}$$

where u and v are the x- and y- components of the perturbation velocity. From (2) and the fact that $L_x \sim \varepsilon L_y$, one can learn that the cross-channel component of perturbation velocity is an order smaller than the along-channel component, i.e., $u \sim \varepsilon v$. With $v \sim \varepsilon V_0$, it becomes that $u \sim \varepsilon^2 V_o$. In the interior region, equations for the x- and y-components of the perturbation velocity are

$$\underset{(\varepsilon^2 R_0)}{u\frac{\partial u}{\partial x}} + \underset{(\varepsilon R_0)}{V_0\frac{\partial u}{\partial y}} + \underset{(\varepsilon^2 R_0)}{v\frac{\partial u}{\partial y}} = \underset{(1)}{-g\frac{\partial \eta}{\partial x}} + \underset{(\varepsilon E_k)}{fv} + \underset{(\varepsilon^2 E_k)}{A\frac{\partial^2 u}{\partial x^2}} + \underset{(\varepsilon^2 E_k)}{A\frac{\partial^2 u}{\partial y^2}} \tag{3}$$

$$\underset{(R_0)}{u\frac{\partial v}{\partial x}} + \underset{(R_0/\varepsilon)}{V_0\frac{\partial v}{\partial y}} + \underset{(R_0)}{v\frac{\partial v}{\partial y}} = \underset{(1)}{-g\frac{\partial \eta}{\partial y}} \underset{(E_k/\varepsilon)}{-fu} + \underset{(E_k/\varepsilon)}{A\frac{\partial^2 v}{\partial x^2}} + \underset{(\varepsilon E_k)}{A\frac{\partial^2 v}{\partial y^2}} \tag{4}$$

where η is the perturbation surface elevation and A is the eddy viscosity coefficient. In (3) and (4), the order of magnitude of each term relative to the Coriolis force is given below in parentheses, except the pressure gradient term. In these estimations, R_o is the Rossby number defined as $R_o = \varepsilon V_0/(fL_x) \sim v/(fL_x)$, and E_k is the Ekman number defined as $E_k = A/(fL_x^2)$. We assume here that $E_k \sim R_o \sim \varepsilon$. This means that, from (4), both the viscosity effect due to the cross-channel variation of velocity and the momentum transport by the basic flow importantly interfere in the velocity perturbation, which is relevant to the assumption of small velocity perturbation arising from eddy viscosity. It also means, from (3), that the y-component of velocity perturbation is in approximate geostrophic balance. Neglecting the terms of order ε or smaller, and eliminating the pressure gradient terms by cross-differentiating result in.

$$V_0\frac{\partial \zeta}{\partial y} = A\frac{\partial^2 \zeta}{\partial x^2} \tag{5}$$

where the relative vorticity ζ $(=\partial v/\partial x - \partial u/\partial y)$ can be approximated to $\zeta = \partial v/\partial x$ to within order ε^2.

It is reasonable to assume that the viscous stress exerting at the outer edges of the interior region is proportional to the current speed of the basic flow, V_0. This sets the boundary conditions of the problem as follows:

$$A\frac{\partial v}{\partial x} = A\zeta = kV_o \quad \text{at } x = x_1$$

$$A\frac{\partial v}{\partial x} = A\zeta = -kV_o \quad \text{at } x = x_2 \tag{6}$$

where k is the constant of proportionality, x_1 is the position of the outer edge of the interior region formed near the left wall of the channel, and x_2 is that corresponding to the right wall of the channel. Since the boundary layers are much narrower than the channel width, x_1 and x_2 are substantially the positions of, respectively, the left and right walls of the channel. Equations (5) and (6) show that the vorticity field in the interior region is governed by a simple diffusion equation. Since the magnitude of relative vorticity, ζ, is expected to be maximum at $x = x_1$ and $x = x_2$, the order of magnitude of ζ is kV_0/A. Since ζ is also of order $\varepsilon V_o/Lx$, it means that $k \sim \varepsilon A/L_x$. For

convenience, non-dimensionalize ζ by kV_o/A, and x and y by L_x. Hereafter, these variables are understood as non-dimensionalized unless otherwise stated. Then (5) becomes

$$\frac{\partial \zeta}{\partial y} = \mu \frac{\partial^2 \zeta}{\partial x^2} \tag{7}$$

where $\mu = A/(L_x V_o) = \varepsilon E_k/R_o$ is the non-dimensional viscosity coefficient with magnitude of order ε. At this point, it may be worthwhile to check to what extent this model can be applied to the Tsushima Current flowing through the Korea Strait. It is reasonable to take $L_x \sim 10^5$ m and $V_o \sim 10^{-1}$ m/sec. The magnitude of A is not quite certain, but the upper limit of A is believed to be about 10^3 m^2/sec because most successful numerical models covering this area employ the value of A smaller than 10^3 m^2/sec (e.g., Seung and Kim, 1993; Kim and Yoon, 1999). These values lead to ε or μ smaller than 10^{-1} which is an acceptable range for the assumption of small viscosity limit. However, for channels with A much larger than 10^3 m^2/sec, this model is no longer valid. Equation (7) indicates that the along-channel length scale (non-dimensional) is of order $1/\mu \sim 1/\varepsilon$, which means, in dimensional form, $L_y \sim L_x/\varepsilon$ as assumed at the outset. The non-dimensional form of (6) is

$$\begin{aligned} \zeta &= 1.0 \quad \text{at } x = x_1 \\ \zeta &= -1.0 \quad \text{at } x = x_2 \end{aligned} \tag{8}$$

Since the maximum of v occurs where $\zeta=0$, Equation (8) indicates that the velocity maxima always present within the channel. For an initial condition $\zeta(x, 0) = \zeta_0(x)$, the solution to (7) and (8) is given (Carslaw and Jaeger, 1959) by

$$\zeta = 1 - \frac{2(x-x_1)}{l} + \frac{2}{\pi} \sum_{n=1}^{\infty} \frac{\{\cos(n\pi)+1\}}{n}$$

$$\sin\left\{\frac{n\pi(x-x_1)}{l}\right\} e^{-\mu n^2 \pi^2 y/l^2} + \frac{2}{l} \sum_{n=1}^{\infty} \sin\left\{\frac{n\pi(x-x_1)}{l}\right\} e^{-\mu n^2 \pi^2 y/l^2}$$

$$\int_{x_1}^{x_2} \zeta_0(x) \left\{\frac{n\pi(x-x_1)}{l}\right\} dx \tag{9}$$

where $l = x_2 - x_1$.

MODEL RESULTS

The solution obtained in the above section is applied to three cases. First, the formation of a single stream core when a uniform stream enters the channel is considered. Next, it is considered that the channel is divided into two sub-channels by a long and narrow island. When a single-cored stream enters into these sub-channels, it is modified into a double-cored stream with a core in each sub-channel. As indicated in (8), stream cores are expected to be formed as soon as the stream enters the channel (or sub-channel). Finally, it is considered that the double-cored stream leaves the island behind. In this case, the stream becomes single-cored again. However, it is not apparent whether the change from double to single core is immediate as in the former two cases. This point will be discussed below in more detail.

Formation of a single-cored stream

Consider a semi-infinite channel where a uniform stream enters from outside. Take a coordinate axis such that $y=0$ coincides with the upstream end of the channel (Fig. 3a). For a given y, $\zeta(x)$ can be obtained straightforwardly by substituting $x_1=-1$, $x_2=1$, $l=2$ and $\zeta_0(x)=0$ into (9). Note that, by substituting these values into (9), ζ(x) approaches asymptotically to -x as y goes to infinity.

Velocity profile in the cross-channel direction, $v(x)$, can be evaluated by integrating $\zeta(x)$ with respect to x. The constant of integration is taken arbitrarily such that $v=0$ at $x=-1$ because we are interested only in the shape of velocity profile. As expected, a broad stream core develops inside the channel immediately after the uniform stream enters the channel (Fig. 4). It then becomes gradually sharper as the stream flows in the downstream direction, approaching asymptotically to the parabolic form corresponding to $\zeta(x) = -x$ infinitely far downstream. In this computation, $\mu=10^{-2}$ is used. For larger value of μ, the stream will approach more rapidly to the asymptotic parabolic form and vice versa, as shown later.

Formation of a double-cored stream

In the presence of an island running in the along-channel direction, a double- cored stream is formed. For simplicity, the island is assumed to lie at $x=0$ and have negligibly small width in x-direction. Let $y=0$ coincide with the upstream end of the island (Fig. 3b). The current entering the sub-channels is assumed to be well adjusted to the channel without the island, i.e., $\zeta_0(x)=-x$. The vorticity ζ(x) is then found separately for each sub-channel as follows. For

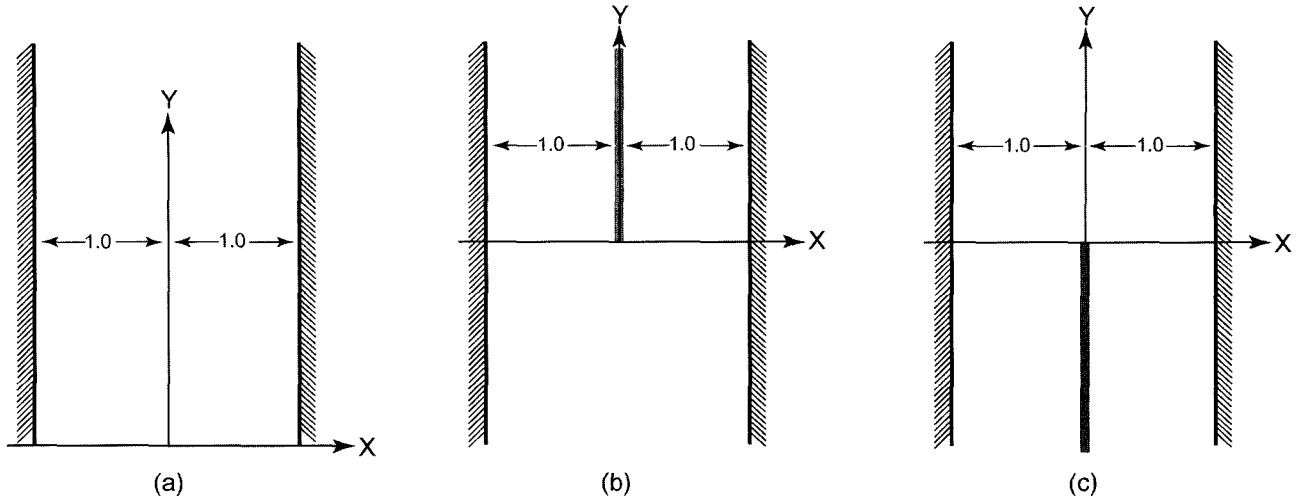

Fig. 3. Three cases where the model result is applied: (a) A uniform current enters into a semi-infinite channel extending from y=0. (b) The current flowing along the channel enters two sub-channels divided by an extremely narrow and semi-infinite island extending from y=0. (c) The currents flowing along the two sub-channels leave the island which ends at y=0.

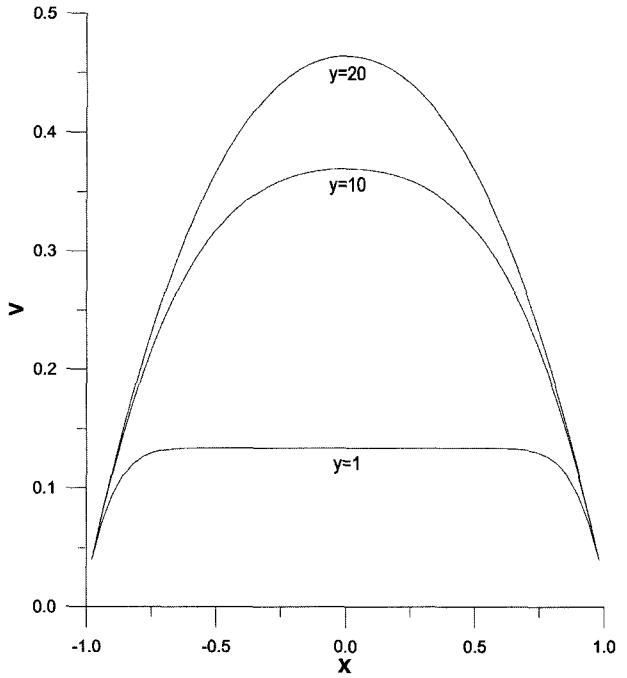

Fig. 4. Along-channel changes of current profiles when a uniform current enters a channel.

the left sub-channel (-1<x<0), the vorticity $\zeta(x)$ is obtained straightforwardly by substituting $\zeta_0(x)$ given above, x_1=-1, x_2=0, and l=1 into (9), and for the right sub-channel (0<x<1), by substituting the same $\zeta_0(x)$, x_1=-1, x_2=0, and l=1 into (9). It can be found that, for sufficiently large y, $\zeta(x)$ becomes asymptotically to -2x-1 for the left sub-channel and to 1-2x for the right sub-channel.

Velocity profiles, $v(x)$, are evaluated by integrating $\zeta(x)$ with respect to x in the similar way as mentioned above. In this case, however, it is assumed that v=0 at x=-1 and at x=1. This is to retain the continuity of the stream profile around the upstream end of the island. Recall that the stream just before entering the sub-channels is in contact with the narrow boundary layers at x=-1 and x=1, but not around x=0.

As expected, a single core begins to be divided into two immediately after the stream enters the sub-channels. Immediately after entering the sub-channels, the stream begins to have two cores on both sides of the island. As the stream proceeds further downstream, these cores slowly move toward the center of each sub-channel. Ultimately, the stream profiles approach toward the asymptotic parabolic forms corresponding to $\zeta(x)$= -2x-1 for the left sub-channel and ζ(x)=1-2x for the right sub-channel (Fig. 5).

Change from a double- to a single-cored stream

Take the coordinate such that y=0 coincides with the downstream end of the island (Fig. 3c). The stream is assumed to be well adjusted to the sub-channels before leaving the sub-channels behind, i.e., $\zeta_0(x)$= -2x-1 for -1<x<0 and $\zeta_0(x)$=1-2x for 0<x<1. For sufficiently large y, $\zeta(x)$ approaches asymptotically to -x, adjusting again to the channel without island. For finite value of y, the vorticity $\zeta(x)$ is obtained straightforwardly by substituting ζ_0 (x) given above, x_1=-1, x_2=1, and l=2 into (9). The velocity profile $v(x)$ is then evaluated from $\zeta(x)$ in the same way as mentioned above.

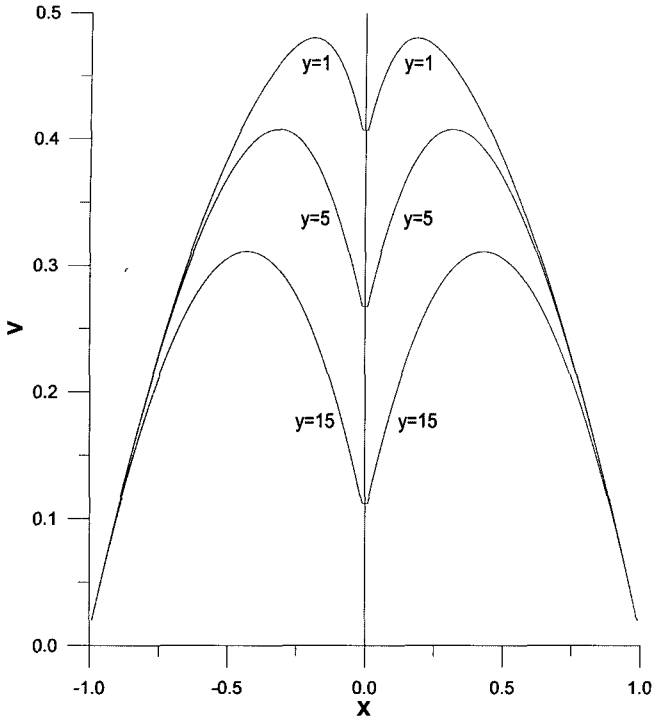

Fig. 5. Along-channel changes of current profiles when a single-cored current enters two sub-channels divided by a long island located at x=0.

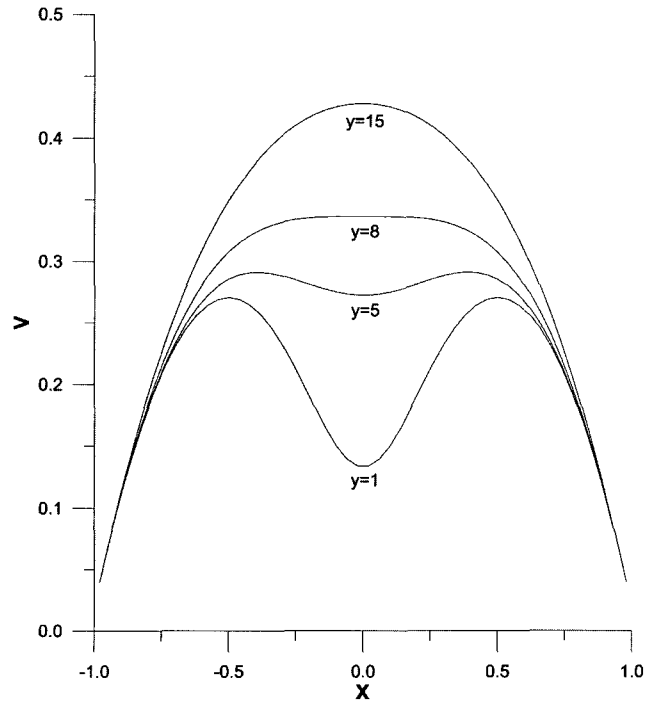

Fig. 6. Along-channel changes of current profiles when the double-cored current leaves the island behind and joins the initial channel.

It is seen that the stream retains its double-cored structure for a significant distance after leaving the island (Fig. 6). A broad single core begins to appear at y=8. At y=15, the stream is very near the asymptotic parabolic form corresponding to $\zeta(x)=-x$. The distance to which the stream retains its double-cored structure depends on the value of μ. For μ=0.1, ten times larger than μ=0.01 considered here, a near-parabolic form of stream profile is already seen at y=8 but for μ=0.001, ten times smaller than μ=0.01, a double-cored stream profile is still seen at y=8 (Fig. 7).

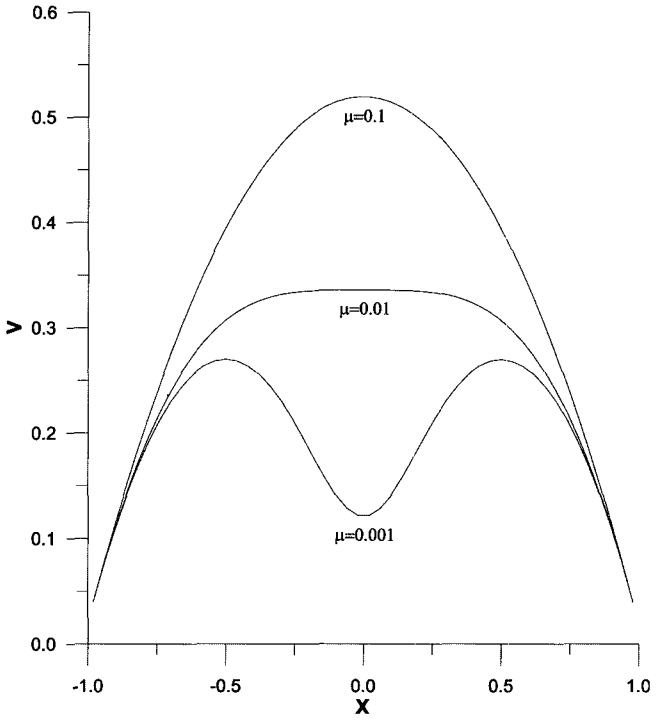

Fig. 7. Current profiles at y=8 after the current leaves the island behind, for three different viscosity coefficients.

CONCLUDING REMARKS

The model proposed above successfully shows the role played by the Tsushima Island in separating the Tsushima Current stream core. Physical explanations can be given as follows. A uniform current becomes to have a stream core when it enters a channel because of lateral eddy viscosity induced by lateral solid boundaries on either sides of the channel. This single core structure is apparent immediately after the current enters the channel. At the beginning, the core is broad but progressively becomes sharper as the current flows downstream. If this current with a single stream core passes an island locating at the center of the channel, two stream cores are formed on each side of the island, by the same reason as a uniform current becomes to have a single core in the channel without island. When this double-cored current leaves the island behind, this shape is retained for a significant

distance before recovering its single-cored structure further downstream. These results indicate that the double-cored Tsushima Current observed just downstream of the Tsushima Island is induced by lateral friction exerted by the Tsushima Island.

It is noted that this model describes only a qualitative aspect of the real problem because it is not known how well the double-cored structure develops on either sides of the Tsushima Island and how much fast the single cored structure is recovered after the Tsushima Current leaves the Tsushima Island behind. This depends largely on the eddy viscosity coefficient μ which is assumed small in this model. For more quantitative analysis in the future, the character of the lateral eddy viscosity should be clarified. Whether the Tsushima Current is barotropic or baroclinic does not matter here because we are concerned only with the lateral variation.

The double-cored structure downstream of the Tsushima Island is expected to be retained for a significant distance especially because the Korea Strait widens rapidly downstream. An interesting question is whether or not the double-cored structure is related with the branching of the Tsushima Current. Traditionally, the branching has been believed to be purely the basin-scale problem, that is, the EKWC is due to the beta-effect (Yoon, 1982a), the NB (Nearshore Branch) is topographically induced (Yoon, 1982b), and the OB (Offshore Branch) is an internal Kelvin wave expression of the summer time volume transport increase (Kawabe, 1982b). On the other hand, there are some different views that the branching is locally generated, either through a channel hydraulic control based on potential vorticity conservation (Cho and Kim, 2000) or through a frictionally-modified vorticity dynamics (Ou, 2001). The branching mechanisms mentioned above are fundamentally different from the mechanism of the stream core separation (or merging) discussed in this paper. Hence, the double-cored structure observed in the downstream of the Tsushima Island, probably induced by the lateral friction exerted by the Tsushima Island, can hardly be related with the branching of the Tsushima Current mentioned above. However, it may be possible that the double-cored stream induced by the effect of lateral friction enhances the branching of the Tsushima Current to some extent.

ACKNOWLEDGEMENTS

This study was supported by grant No. R01-2001-000-00076-0 from the Korea Science and Engineering Foundation.

REFERENCES

Carslaw, H. S. and J. C. Jaeger, 1959. Conduction of heat in solids. Oxford at the Clarendon Press, 510 pp.

Cho, Y.-K. and K. Kim, 2000. Branching mechanism of the Tsushima Current in the Korea Strait. *J. Phys. Oceanogr.*, **30**: 2788–2797.

Egawa, T., Y. Nagata and S. Sato, 1993. Seasonal variation of the current in the Tsushima Strait deduced from ADCP data of ship - of - opportunity. *J. Oecanogr.*, **49**: 39–50.

Isobe, A., S. Tawara, A. Kanekoand M. Kawano, 1994. Seasonal variability in the Tsushima Warm Current, Tsushima-Korea Strait. *Cont. Shelf Res.*, **14**: 23–35.

Katoh, O., 1994. Structure of the Tsushima Currentin the southwestern Japan Sea. *J. Oceanogr.*, **50**: 317–338.

Katoh, O., K. Teshima, K. Kubota and K. Tsukiyama, 1996. Downstream transition of the Tsushima Current west of Kyushu in summer. *J. Oceanogr.*, **52**: 93–108.

Kawabe, M., 1982a. Branching of the Tsushima Current in the Japan Sea, Part I. Data analysis. *J. Oceanogr. Soc. Japan*, **38**: 95–107.

Kawabe, M., 1982b. Branching of the Tsushima Current in the Japan Sea, Part II. Numerical experiment. *J. Oceanogr. Soc. Japan*, **38**: 183–192.

Kim, C.-H. and J.-H. Yoon, 1999. A numerical modeling of the upper and the intermediate layer circulation in the East Sea. *J. Oceanogr.*, **55**: 327–345.

Miita, T. and Y. Ogawa, 1984. Tsushima Currents measured with current meters and drifters. In: Ocean Hydrodynamics of the Japan and East China Seas, T. Ichiye, Ed., Elsevier, pp 67–76.

Mizuno, S., K. Kawatate, T. Nagahama and T. Miita, 1989. Measurements of east Tsushima Current in winter and estimation of its seasonal variability. *J. Oceanogr. Soc. Japan*, **45**: 375–384.

Ou, H. W., 2001. A model of buoyant throughflow : with application to branching of the Tsushima Current. *J. Phys. Oceanogr.*, **31**: 115–126.

Seung, Y. H. and K. Kim, 1993. A numerical modeling of the East Sea circulation. *J. Oceanol. Soc Korea*, **28**: 292–304.

Teague, W. J., G. A. Jacobs, H. T. Perkins, J. W. Book, K.-I. Chang and M.-S. Suk, 2002. Low-frequency current observations in the Korea/Tsushima Strait. *J. Phys. Oceanogr.*, **32**: 1621–1641.

Toba, Y., K. Tomizawa, Y. Kurasawa and K. Hanawa, 1982. Seasonal and year- to- year variability of the Tsushima-Tsugaru Warm Current system with its possible cause. *La Mer*, **20**: 41–51.

Yoon, J.-H., 1982a. Numerical experiment on the circulation in the Japan Sea, Part I: Formation of the East Korean Warm Current. *J. Oceanogr. Soc. Japan*, **38**: 43–51.

Yoon, J.-H., 1982b. Numerical experiment on the circulation in the Japan Sea, Part III: Formation of the Nearshore Branch of the Tsushima Current. *J. Oceanogr. Soc. Japan*, **38**: 119–124.

Yi, S. U., 1966. Seasonal and secular variations of the water volume transport across the Korea Strait. *J. Oceanol. Soc. Korea*, **1**: 7–13.

Yi, S. U., 1970. Variations of oceanic condition and mean sea level in the Korea Strait. In: The Kuroshio: A symposium on the Japan Current, J. C. Marr, Ed., East-West Center Press, pp 125–141.

Manuscript received February 3, 2003
Revision accepted May 12, 2003
Editorial handling: Yign Noh